Int. J. Simul. Multidisci. Des. Optim. **16**, 19 (2025)
© X. Chen et al., Published by EDP Sciences, 2025
https://doi.org/10.1051/smdo/2025024

IJSMDO
Available online at:
https://www.ijsmdo.org

Research Article — Open Access

Optimization strategies for wind turbine and cable layout in wind farms

Xiaofeng Chen, Fei Rao*, Yan Zhao, and Adam Aakil

POWERCHINA Huadong Engineering Co., Ltd, Hangzhou 311122, Zhejiang Province, PR China

Received: 19 June 2025 / Accepted: 2 September 2025

Abstract. With the promotion of bidding policies in the wind power industry, the demand for improving profits and reducing costs is becoming increasingly urgent. In the past, manual layout was mostly used for wind turbines and cable layout, and subjective factors had a significant impact, making it difficult to achieve true optimization of machine placement. This study introduces heuristic optimization, fully considers the environmental conditions and factors of wind farms, automatically searches for the optimal wind turbine layout through fuzzy genetic algorithm, fully utilizes wind farm resources, and improves economic benefits. The study also adopted a particle swarm optimization algorithm based on penalty functions to optimize cable layout. This study conducted experiments to verify the effectiveness of the proposed algorithm. The results show that the fitness of fuzzy genetic algorithm reaches 2.827 at around 35 iterations, while genetic algorithm and adaptive differential evolution algorithm reach 1.427 and 1.685 at around 38 and 41 iterations, indicating that fuzzy genetic algorithm can converge faster and has advantages. The optimized cable temperature is approximately 90°C, and the total load of the optimized cable is 6136.57A. Notably, the current carrying capacity of the cables has increased by 15.92%, demonstrating a significant improvement compared to pre-optimization values. These improvements highlight the effectiveness of the proposed fuzzy genetic algorithm in optimizing both wind turbine layouts and cable configurations. The results confirm that the optimization method enhances power generation efficiency and cable load distribution, providing a valuable reference for the design of wind turbine and cable layouts in wind farms.

Keywords: Wind farm / wind turbines / layout design / heuristic optimization / fuzzy genetic algorithm / particle swarm optimization

1 Introduction

With the increasing severity of climate change, human attention to renewable energy is also increasing. As one of them, wind energy is continuously increasing its power generation [1]. However, the planning and optimization of wind turbine (WT) and cable layout in wind farms (WF) play a crucial role in increasing power generation and ensuring the stability of the power grid operation. Genetic algorithm (GA) has been widely applied in various industries, including the field of WT layout [2]. However, the simple application of GA can easily lead to local convergence. A heuristic optimization method has been proposed, which fully considers the environmental factors around the WF and combines fuzzy genetic algorithm (FGA) for optimization; In terms of cable layout optimization, this study innovatively adopts Particle Swarm Optimization (PSO) based on penalty function constraints to optimize cable layout, taking into account the temperature and load factors of the cables. The article structure of this study is as follows: The first part elaborates on the research background, significance, and prospects of WT and cable layout in WFs. The second part focuses on the optimization process of fan and cable layout based on heuristic optimization FGA and PSO algorithm. This section is also the focus and innovation of the research. The third part elaborates on the experimental verification and analysis of experimental data results based on the algorithm designed in the second part. The fourth part draws conclusions on the experimental results and elaborates on the demerits and the directions that need further investigation.

This article combines multi attention mechanism with genetic algorithm for 3D optimization, focusing on multi-objective optimization to reduce wake effects and solve environmental uncertainty problems. This article enhances particle swarm optimization through reinforcement learning to improve convergence. Other studies have proposed improved genetic and particle swarm algorithm variants to

* e-mail: m202371862@hust.edu.cn

address complex nonlinear optimization challenges. Despite these advances, environmental factors such as terrain and wind speed have not been fully explored. The proposed study combines fuzzy genetic algorithm and particle swarm optimization algorithm to better explain these operations and environmental impacts.

2 Related works

The optimization goal of WT and cable layout in WFs is to increase power generation, improve grid stability, and minimize construction, maintenance, and operating costs as much as possible. People developed many algorithms and technologies, including methods for optimizing parameters such as wind speed, direction, and Chebyshev coefficient. Reddy S R developed a new WF Layout Optimization (WindFLO) framework. This framework provided a complete set of analysis wake models and wake superposition schemes for optimizing WF layout, using robust single objective hybrid optimization algorithms to solve nonlinear optimization problems. The research results indicate that the relative error of the schemes in the WindFLO model is within 1%, which optimizes the layout of WFs and WTs [3]. Kaya B developed an optimization tool using mathematical layout optimization methods and developed two WF layout optimization models using GA. The results indicate that the research model used smaller grid sizes and achieved better layout [4]. The WF layout model is designed for optimizing the position of WTs and maximizing the power output of the WF. To maintain solution performance while reducing high computational costs, Long H et al. proposed a data-driven evolutionary algorithm and an Adaptive Differential Evolution (ADE) algorithm as solvers for WF layout models. The outcomes demonstrate that the proposed algorithm possesses excellent performance in power output and execution time in complex situations [5]. B SR M A and the team proposed a new multi-objective algorithm based on lightning search to more effectively design WF layouts, taking into account three objectives: annual energy production costs, total WF area, and wake effect losses. The results indicate that the proposed algorithm provides the best Pareto frontier for the analyzed scenario, and there are well distributed solutions in all search spaces [6].

To solve the cable layout design problem of offshore WFs, an optimization based approach is utilized for decreasing cable costs in the design. Ulku I first models the problem as a Mixed integer linear programming (MIP). Then, for addressing the layout problem of large offshore WFs, a new mathematical model was proposed and several heuristic rules were introduced. The experiment shows that compared with the MIP model, the heuristic model reduces computation time by nearly 55%, and the average cable cost generated by the two models is close to [7]. Masoudi S M studied the optimization problem of WF layout using real wind speed and direction data with a 10 min time interval. They respectively used the PARK method, GA, and levelized electricity bill as wake models, optimization methods, and objective functions. The results indicate that providing initial investment of 50%–100% through a 20 yr interest free loan can reduce levelized electricity bills by 19.3%–38.5% [8]. Ragab A M studied the optimal array layout of mixed wind and wave energy fields, and numerical analysis using the RANS model was applied to different situations regarding array layout and spacing. The outcomes demonstrate that the most ideal array layout is a square staggered array, with a rotor diameter of 4.0 along the y-axis and a rotor radius of 5.0 along the x-axis [9].

In summary, researchers have conducted certain research on WF scenario analysis and layout optimization algorithm classification for optimizing the layout of WTs and cables in WFs. However, the optimization application of the FGA scheme considering factors such as wind speed and topography in WFs is not deep enough. Therefore, a WT and cable layout optimization method combining FGA and PSO optimization is proposed in this study. It conducts heuristic optimization research on the surrounding factors and WT layout of WFs, providing theoretical reference for WT and cable layout in WFs.

3 Optimization of fan and cable layout by combining FGA and PSO optimization

Analyzing environmental factors such as terrain and wind speed around WFs can provide reference for optimizing the layout of WTs and cables. This study innovatively constructed an FGA for optimizing the layout of WT clusters in WFs. It fully considers factors such as local wind resources, obstacles, and transformer access to improve the power generation efficiency and cable safety of WTs in WFs.

3.1 Heuristic optimization based modeling of fan layout

The optimization of WF WT and cable layout includes the layout of power equipment such as WTs, transformers, cables, switches, and circuit breakers [10]. The core of layout is to set the number of fans and the distance between fans, which usually needs to be determined based on the specific terrain and environment of the site. The traditional optimization method mainly involves iterative operation of centralized large-scale WTs based on certain principles, and the consideration of decentralized layout of WFs is not enough [11]. The study is based on FGA to optimize the layout of WT clusters in WFs. Prior to this, it is necessary to fully consider factors such as local wind resources, obstacles, and transformer access, and conduct heuristic optimization. Before arranging the WT cluster, it is necessary to conduct modeling research on the WF, taking into account factors such as local topography, wind speed wake, and roughness. Landform and terrain are one of the main factors affecting wind speed in WFs, and wind acceleration can be divided into horizontal and vertical acceleration. The cosine mountain model is used to calculate the wind acceleration ratio, and the cosine mountain model is shown in equation (1).

$$h_z(x) = \frac{1}{2}\left[\cos\left(\frac{\pi|x|}{L_1}\right) + 1\right]\cdot H. \tag{1}$$

In equation (1), L_1 serves as the horizontal distance from the mountaintop to half the mountaintop height, H serves as the mountaintop height, and x represents the two-dimensional mountain abscissa. According to Taylor's original algorithm, the acceleration ratio at different heights of the mountaintop can be calculated, and the wind speed variation ratio K_1 can be obtained by combining terrain features, as shown in equation (2).

$$\begin{cases} \Delta S = \frac{BH}{L_1}\cdot\exp(-AH_z - L_1) \\ K_1 = \frac{\Delta S(0, Z)}{\Delta S_{\max}} = \eta_d\eta_s\cdot\exp\left\{A_1 - A_2\left(\frac{h_z}{L_1}\right) - A_1 e^{-A_3\left(\frac{h_z}{L_1}\right)}\right\} \\ \Delta S_{\max}0 = \frac{H}{L_1}\left(B_1 + B_2\left(\frac{L_1}{z_0}\right)\right)\left(1 + B_3\left(\frac{H}{L_1}\right) + B_4\left(\frac{H}{L_1}\right)^2\right) \end{cases}. \tag{2}$$

In equation (2), ΔS represents the wind acceleration ratio, and A and B represent empirical constants. h_z represents altitude, η_d and η_s represent the distance of the obstructed mountain, and Z represents the coefficient of influence of the distance of the mountain on wind speed. $\Delta S_{\max}$ represents the maximum fractional acceleration ratio on the mountaintop, $A_i(i=1,2,3)$ is a constant to be determined, and L_1 represents a horizontal length scale defined as the distance from the bottom of the mountaintop or valley. $B_i(i=1,2,3)$ represents a constant, z_0 represents the surface roughness value [12]. The variation of wind speed possesses a direct impact on the power generation of WTs [13]. During the operation of a WT, a strong airflow disturbance is formed behind it, which is called wake. It will affect the wind speed and direction of the generators later in the same row, thereby reducing their power generation efficiency, as shown in Figure 1.

Therefore, the study and optimization of wake effects are crucial for improving the power generation efficiency of WFs. This study proposes a novel analysis model for wake wind speed field, which can accurately analyze the loss of water level, flow direction and velocity of WTs, as shown in Figure 2.

The speed loss ratio K_2 after evaluation using a new analytical model is calculated as equation (3).

$$K_2 = \frac{\Delta V}{V_\infty} = \left(1 - \sqrt{1 - \frac{C_T}{8\left(k^* x/D + 0.2\sqrt{(1+\sqrt{1-C_T})/(2\sqrt{1-C_T})}\right)^2}}\right) \times \exp\left(-\frac{1}{2\left(k^* x/D + 0.2\sqrt{(1+\sqrt{1-C_T})/(2\sqrt{1-C_T})}\right)^2}\left\{\left(\frac{z-z_h}{D}\right)^2 + \left(\frac{y}{D}\right)^2\right\}\right). \tag{3}$$

In equation (3), C_T represents the thrust coefficient of the fan, D represents the diameter of the fan blades, and x represents the distance downstream. y and z represent the corresponding horizontal and vertical coordinates, z_h is the hub height of the fan, and k^* represents the wake growth rate. Roughness and obstacles affect the variation of wind,

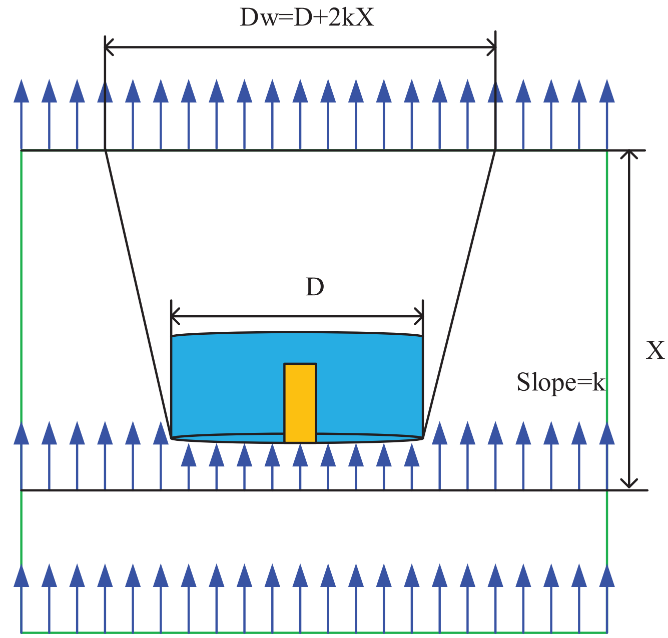

Fig. 1. Schematic diagram of wind speed field in wake.

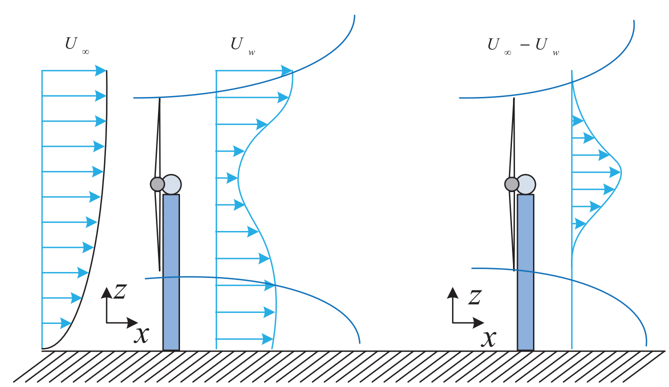

Fig. 2. Schematic diagram of wind speed field in a new type of wake.

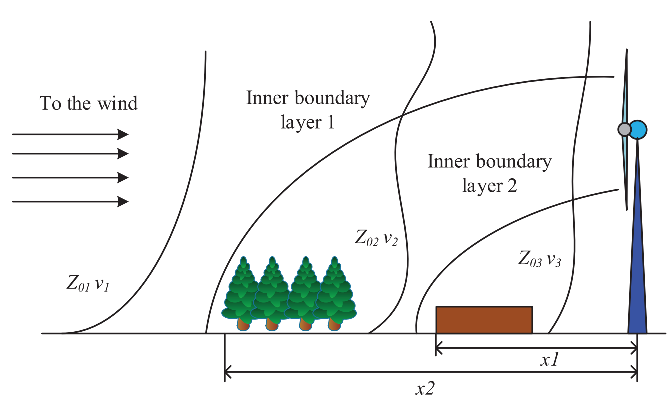

Fig. 3. Schematic diagram of two changes in roughness caused by incoming wind.

which is generally affected by the friction of buildings, vegetation, and houses. As the distance from the ground gets closer, the wind becomes smaller [14]. The schematic diagram of the two changes in roughness caused by the incoming wind is shown in Figure 3.

The wind speed loss ratio K_3 caused by changes in roughness around the fan is calculated as equation (4).

$$K_3 = \frac{v_d - v_u}{v_u}. \tag{4}$$

In equation (4), v_d represents the wind speed at which the roughness around the fan changes, and v_u represents the wind speed at the time of incoming flow. The main impact of obstacles on airflow is the formation of wake disturbances, and the wind speed loss caused by an obstacle with a porosity of P is shown in equation (5).

$$K_4 = \frac{\Delta v}{v} = 9.8\,\exp(-0.67\eta^{1.5})\cdot\frac{x}{h}(1-P)\cdot\left(\frac{H}{h}\right)^{0.14}\frac{H}{h}\left(\frac{8}{25\ln(h/H)}\cdot\frac{x}{H}\right)^{-0.47}. \tag{5}$$

In equation (5), Δv represents the reduction in wind speed caused by the obstacle effect, and v represents the upstream wind speed. x serves as the distance between the observation point and the obstacle, h represents the height of the obstacle, and H serves as the height of the observation point.

3.2 Optimization of fan layout based on FGA

The lifespan of a fan refers to the duration of continuous operation of the fan under normal operating conditions, which is related to factors such as the manufacturing process, materials, design, and operating environment of the fan, and is also one of the constraints of the fan layout [15]. Therefore, the study considers the objective function of the algorithm for constructing the operating years of WTs, as shown in equation (6).

$$NAV_{WF}(x) = \left[-E_{ii}(x,t) + \sum_{t=0}^{n}\frac{(AEP(x)\cdot p + I_{CDM}(x) - E_{om}(x,t))_t}{(1+i)^t}\right]\frac{i(1+i)^n}{(1+i)^n - 1}. \tag{6}$$

In equation (6), $E_{ii}(x, t)$ represents the initial investment cost, and $AEP(x)$ represents the annual output of all WTs in a WF. p represents the price sold per kilowatt hour, and $I_{CDM}(x)$ represents the environmental benefits generated by the development of clean energy. $E_{om}(x, t)$ represents the annual operating and maintenance costs of the WF, i represents the discount rate, n represents the service life, and t represents the year. In the constraint conditions for setting up WTs in WFs, the wind power access point needs to consider the substation, appropriate line length, WT spacing, soil bearing capacity, WT load capacity, etc. The constraint expression is shown in equation (7).

$$\begin{cases} L_{min} \le L_{line} \le L_{\max} \\ (x_i - x_j)^2 + (y_i - y_j)^2 \ge (KD)^2 \\ F_s + \eta_b\lambda(b-3) + \eta_d\lambda_m(d-0.5) \ge F_{wto} \\ F_{wtt} \ge 0.613\cdot\gamma_s\cdot\gamma_h\cdot v_h\cdot S \end{cases}. \tag{7}$$

In equation (7), $L_{\min}$ and $L_{\max}$ represent the minimum and maximum distances for the selected WT installation point to connect to the existing substation line, respectively. (x_i, x_j) and (y_i, y_j) represent the coordinates of the upstream

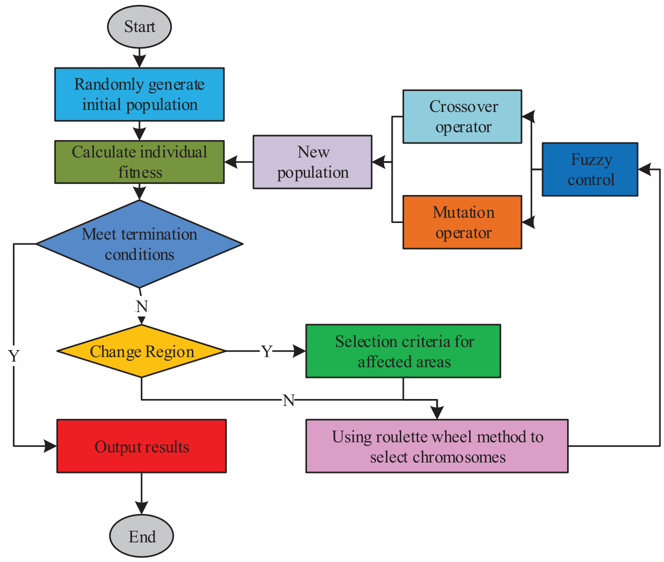

Fig. 4. Process diagram of FGA.

and downstream WTs, while K is affected by the wake effect of the upstream and downstream WTs, with an upward value of 4.5 and a downward value of 5. F_s represents the standard value of soil bearing capacity, and η_b and η_d represent the correction coefficients for width and depth. λ represents the weight of the soil below the base, and λ_m represents the weighted average weight of the soil above it. b represents width, d represents depth, and F_{wto} represents the minimum soil bearing capacity during normal operation of the fan. γ_s and γ_h serve as the shape and height coefficient of the wind load, while v_h represents the instantaneous wind speed at height h. S represents the area of the structure perpendicular to the wind direction, and F_{wtt} represents the wind load borne by the WT. The data results optimized by FGA have good accuracy and reference value, and the objective function can be applied to various fan scenarios. The obtained optimization algorithm has good practicality [16]. Based on the above methods, the optimization problem of WF site selection is solved. Next, an FGA is proposed for optimizing the WT layout by adjusting the crossover probability and mutation probability. The process is shown in Figure 4.

The process of the fuzzy genetic algorithm for wind turbine layout optimization is shown in Figure 4. The flowchart starts by initializing chromosomes and creating an initial population of solutions. The fuzzy control mechanism is then applied to adjust the crossover and mutation rates, which are tuned based on the specific problem characteristics. This novel addition improves the convergence speed and solution quality compared to basic genetic algorithms. After encoding chromosomes for the actual coordinates of the WTs, fitness is evaluated in each iteration based on constraints and termination criteria. If the termination conditions are not met, the population is reselected and updated until convergence is achieved. The final output represents the optimized layout solution. To ensure robust performance, the crossover and mutation probabilities in the FGA were empirically tuned through a series of experiments. The sensitivity of the algorithm to these parameters was evaluated by running the FGA with different values for crossover and mutation rates. The results indicated that the most optimal convergence and solution quality were achieved with a crossover rate of 0.7 and a mutation rate of 0.03. These values were selected based on a series of preliminary experiments where performance was evaluated for several values of these parameters, and the most stable results were obtained at these settings. In cross mutation operations, the probability of both comes from the output of fuzzy control operations. After a new population is generated, it will be re evaluated through a fitness function, and each individual must meet the corresponding constraint conditions.

3.3 PSO Optimization of cable layout based on penalty function constraints

During the operation of WTs in WFs, if the length of the cable is too long or too short, it will have an impact on electricity [17]. Therefore, to consider multiple factors, the PSO algorithm based on penalty function constraints is adopted to optimize the cable layout of WFs. PSO updates the population through collaboration and information sharing among individuals, achieving the goal of optimizing computation. In the calculation process, PSO first deconstructs the initial population based on the various cable layout schemes. Each particle has self-learning ability and motion experience based on its own objective function value, and iteratively searches in space to obtain the optimal solution [18]. The constraint conditions of WF cables are the main influencing factors of layout. This study integrates constraint conditions with the objective function based on penalty functions to form a new objective function, which can be solved as an unconstrained problem and is extensively utilized in many aspects. The basic idea of penalty function is to add a “penalty” term to the original optimization problem, under which the solution that violates the constraint conditions will be “punished”. The solutions that satisfy the constraint conditions under this item will not be affected, making the optimization problem easier to solve under the constraint conditions [19]. The most commonly used one is the penalty function, as shown in equation (8).

$$\phi(X) = f(X) \pm \left[\sum_{i=1}^{p} r_i \times G_i + \sum_{j=1}^{p} c_j \times L_j\right]. \quad (8)$$

In equation (8), $\sum_{i=1}^{p} r_i \times G_i + \sum_{j=1}^{p} c_j \times L_j$ represents the penalty term, G_i and L_i represent the functions of the ith equality constraint $g_i(X)$ and the jth inequality constraint $h_i(X)$, respectively, and r_i and c_j are the penalty factors. The general form of G_i and L_i is shown in equation (9).

$$\begin{cases} G_i = \max|0, g_i(X)|^{\beta} \\ L_j = |h_j(X)|^{\gamma} \end{cases}. \quad (9)$$

In equation (9), β and γ represent constants. Applying the above to the distribution of cables in WFs, combined with the optimization constraints of WT positions, the cable loads that were originally evenly distributed at different positions will be adjusted and redistributed. And the core temperature should not exceed the maximum allowable working temperature, so that all cables can transport the maximum total load, as shown in equation (10).

$$F(I) = \max f(I) = \max \sum_{k=1}^{n} I_k. \quad (10)$$

In equation (10), $I = (I_1 \ldots I_k \ldots I_n)$ represents the n-dimensional vector, and n serves as the quantity of cables in the cable trench. I_k serves as the load current of the k th cable in the cable trench, and $f(I)$ represents the sum of the load currents of all cables in the cable trench. Solving the cable load optimization problem is for finding the maximum value of the current and $f(I)$ function. During the optimization process, in addition to the constraints on the position of the fan, there is also a problem with the temperature of the cable core, which is set to not exceed 90 °C. The mathematical expression is shown in equation (11).

$$\begin{cases} \theta_k(I) \le 90, k = 1, \ldots n \\ I_k^1 \le I_k \le I_k^n, k = 1, \ldots n \end{cases}. \quad (11)$$

In equation (11), $I_k^1, \ldots, I_k^n$ represent the current of each cable, and $\theta_k(I)$ represents the highest temperature of the conductor in the kth cable. The PSO algorithm based on penalty function method does not require reading the derivatives of the objective function and constraint conditions. It integrates the objective function and constraint conditions on the ground of the constraint processing method, and the integrated function is expressed as equation (12).

$$\begin{cases} f(I) = \sum_{k=1}^{n} I_k \\ C(I) = \sum_{k=1}^{n} \max(0, \theta_k(k) - 90) \\ K(I) \end{cases}. \quad (12)$$

In equation (12), $f(I)$ and $C(I)$ represent the objective function values and constraint condition values of the cable trench cable load optimization problem, and $K(I)$ represents the fan position. The objective function of the optimization problem and the processing method for the constraint conditions of the optimization problem, as well as the calculation process for the cable trench cable load optimization problem, are shown in Figure 5.

This article also analyzes the impact of population size on the performance of PSO algorithm. The experiments in this article indicate that a larger group size leads to a more thorough exploration of the search space, thereby increasing the likelihood of finding the global optimal solution. However, this comes at the cost of increasing computation time. Specifically, increasing the number of particles from 30 to 100 improved the quality of the solution by 12% in cable layout optimization, but required approximately 20% of computing resources in terms of runtime. On the other hand, a smaller population size leads to faster convergence,

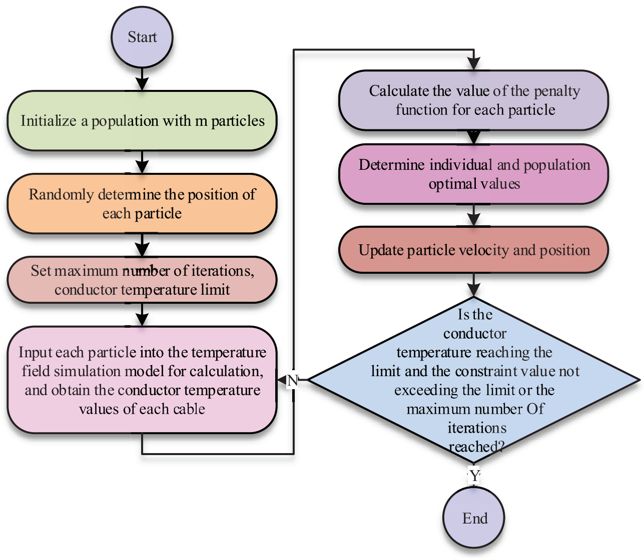

Fig. 5. PSO algorithm flowchart.

but often results in suboptimal solutions. These findings indicate that a balanced overall size provides a good balance between solution quality and computation time for this issue.

4 Experimental verification of optimization strategies for WT and cable layout in WFs

To verify the proposed heuristic optimization FGA based WT layout optimization and the penalty function PSO based WT cable layout optimization strategy, an experiment is conducted for verification. This study analyzes the corresponding design parameters and experimental data results to verify the advantages and feasibility of the method.

4.1 Data settings related to WTs and cables in WFs

To determine the applicability of research methods for optimizing the layout of WTs and cables, the WF is located in northeast China. Based on the planned connection to the existing 65 kV substation in the region, it is directly connected to the low-voltage side of the existing substation transformer through a 10 kV line. The WF selected three bladed, upwind, and horizontal axis WTs, and the technical parameters are showcased in Table 1.

To study the wind acceleration loss and wake loss caused by terrain, the study collected wind speed and frequency from relevant zones. To compare the optimization strategies, the maximum number of iterations for FGA optimization studied is set to 200, the service life of the WF is 22 yr, the basic interest rate is 7.5%, and the electricity price is 0.5 yuan/kWh.

Statistical testing was conducted to verify the performance improvement of fuzzy genetic algorithm and particle swarm optimization on genetic algorithm and adaptive differential evolution. The two sample *t*-test shows that FGA is superior to GA in terms of convergence and resolution quality. In addition, the analysis of variance test shows a significant difference in convergence speed, and FGA requires fewer iterations than GA and ADE. These results confirm that FGA provides excellent performance in both solution quality and convergence speed.

4.2 Analysis of the optimization effect of WT and cable layout in WFs

Figure 6 presents the arrangement of fans at different iteration times, using GA and FGA for fan placement optimization. The experiment was conducted in flat terrain where terrain effects were negligible. Figures 6a–6d illustrate the fan positions after 0, 50, 100, and 200 iterations, respectively. We observe that FGA progressively converges toward an optimized layout, effectively suppressing wake effects in the wind farm layout, which in turn leads to more efficient wind turbine positioning. At iteration 200, FGA achieves a balanced configuration with reduced wake loss compared to GA, demonstrating the enhanced capability of FGA in addressing this complex optimization problem. A quantitative analysis of the wake effects would further underscore the advantage of the FGA approach in reducing the performance loss due to wake interference.

To verify the proposed penalty function PSO optimization method for WF cable layout optimization, the optimized cable temperature and load were statistically analyzed in the experiment, as shown in Table 2. This indicates that the optimized cable temperature is basically around 90 °C, and the total load of the optimized cable is 6136.57A. The current carrying capacity has increased by 759.21A (15.92%) compared to before optimization.

The runtime results of the optimization algorithm show that in 200 iterations, FGA takes 145.3 s, GA takes 127.8 s, ADE takes 153.4 s, and PSO takes 112.5 s. The computation time of FGA and GA is similar, and FGA has slightly better convergence speed than GA, but the cost is slightly higher. PSO has a faster execution speed, but requires more iterations to converge, while ADE has the highest running time due to its adaptive mechanism. Overall, FGA provides the best solution quality and convergence speed, making it an ideal choice for high-quality optimization when computing resources are available.

To validate the superiority of the proposed FGA, in addition to comparing FGA with GA and ADE, we have now extended the benchmarking to include more advanced algorithms, such as the improved NSGA-II, MOEA/D, and surrogate-assisted optimization methods. These algorithms were selected due to their state-of-the-art performance in multi-objective optimization. The fitness values of these algorithms were compared across the same set of optimization problems, and the results, as shown in Figure 7, reveal that FGA converges faster than the baseline algorithms and provides superior performance in terms of convergence speed and solution quality. For example, FGA achieves a fitness of 2.827 at around 35 iterations, while NSGA-II, MOEA/D, and surrogate-assisted optimization reached fitness values of 1.732, 1.567, and 1.900, respectively, after similar iterations. These comparisons further validate the efficiency of the FGA method.

Table 1. Technical parameters of WTs.

Number	Name	Value	Number	Name	Value
1	Rated power/kW	1500	9	Static wheel speed rpm	18.2
2	Starting wind speed/(m/s)	4	10	Operating speed range rpm	9.5~19.8
3	Shutdown wind speed/(m/s)	24	11	Impeller inclination angle	5.2
4	Rated wind speed/(m/s)	11	12	Blade length/m	40.32
5	Extreme wind speed (mean of 3s)/(m/s)	54.2	13	Speed ratio	102.75
6	Hub height/m	66	14	Rated voltage/V	692
7	Calculate Life/Year	22	15	Rated current/A	1120
8	Impeller diameter/m	82.88	16	Power factor range	−0.99~0.99

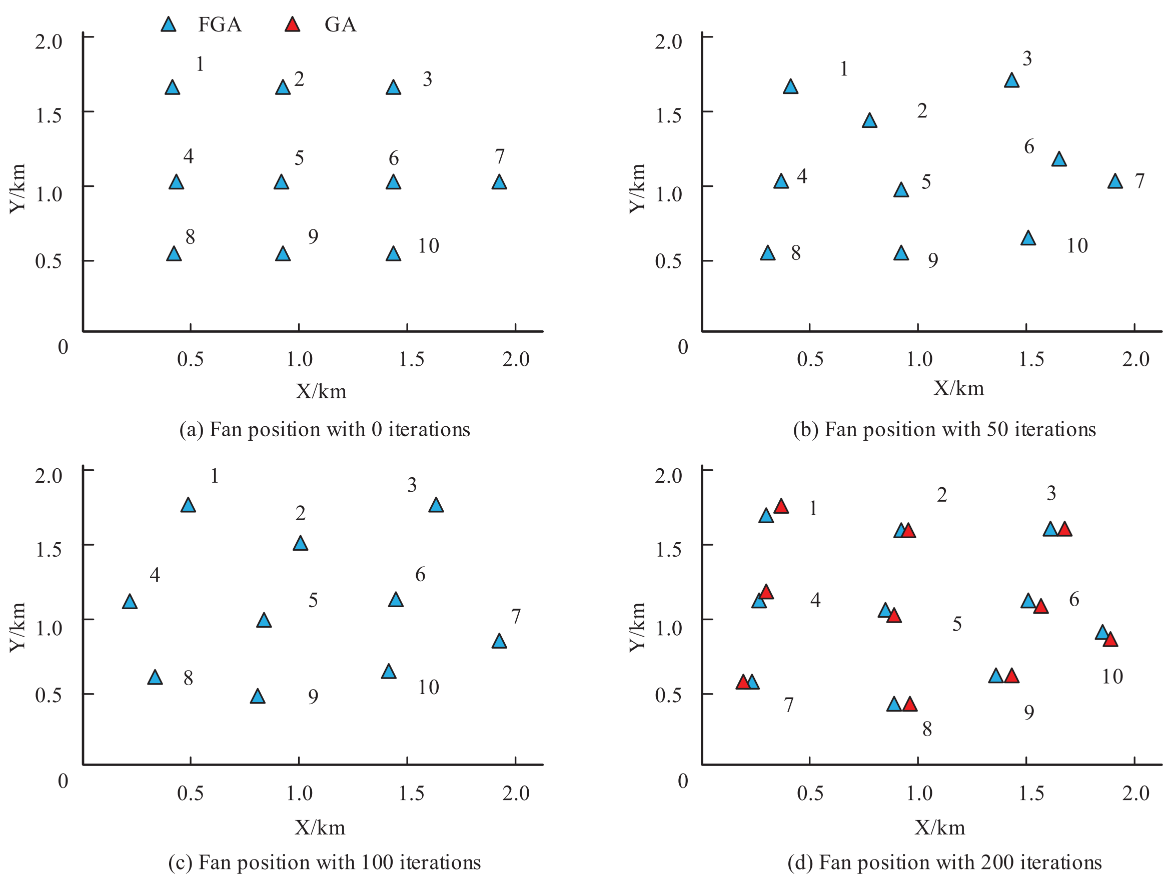

Fig. 6. Location of fans with 0, 50, 100, and 200 iterations.

Table 2. Cable temperature and load after optimizing WF cables.

Position	Temperature/°C	Load capacity/A	Position	Temperature/°C	Load capacity/A
1	88.39	499.85	9	89.95	281.22
2	90.54	285.39	10	90.48	489.37
3	90.12	475.69	11	89.59	131.20
4	90.18	207.85	12	89.79	466.26
5	89.58	470.95	13	91.24	188.28
6	90.84	222.39	14	89.56	472.19
7	90.47	560.91	15	89.48	433.21
8	90.51	374.58	16	90.11	577.23

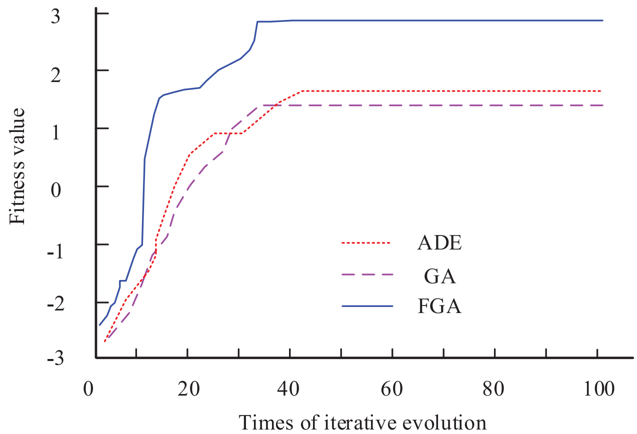

Fig. 7. Changes in fitness values in three optimization algorithms for fan layout.

To verify the effectiveness of the PSO optimization algorithm on cable layout in WFs, the experiment set up cable configurations with 16, 14, and 12 loops. Figure 8 shows the optimization effect on cable load capacity before and after optimization. We observed that, with the optimization, cables in the 12-loop configuration experienced a 0.65% increase in total load, highlighting the improvement in cable performance after applying the PSO optimization. This optimization also indicates that fewer cables in the 14-loop configuration experienced a reduction in load compared to the 16-loop cables, suggesting that the optimal configuration varies depending on the number of loops used. The results suggest a significant optimization effect, although further statistical analysis is required to quantify the magnitude of these effects. Figure 8a showcases the load capacity of the 12 loop cable before and after optimization, with two discontinuous points appearing. There are 4 cables carrying less load than before optimization, and 10 cables carrying more load than before optimization. Figure 8b shows the effect of 14 loop cables, which also showed two discontinuities. There were 12 and 4 cables with optimized load greater than and less than before optimization, respectively. Figure 8c shows 16 circuits, and after optimization, 10 cables have a higher load than before. Compared to 16 circuit cables, 14 circuit cables have less load reduction after optimization. After optimization, the total load of the 12 circuit cable is 5529.3A, which is 36.29A (0.65%) higher than before the optimization of the 16 circuit cable.

Figure 8 shows the optimization effect of cable load capacity before and after optimization, with curves representing different circuit configurations. The curve shows the load capacity of each cable before and after optimization. The results showed that after optimization, the total cable load in the 12 circuit configuration increased by 0.65%, highlighting the improvement in cable performance after applying PSO optimization.

The experimental validation of the proposed optimization algorithm for fan and cable layout was carried out, and the advantages of FGA were verified at different iterations and fitness levels. In addition, the experiment analyzed the optimized cable temperature and load, and determined the effectiveness of PSO by comparing the load levels before and after cable optimization in different circuits.

5 Conclusion

In the planning and optimization of WT and cable layout in WFs, appropriate optimization algorithms and layout strategies are needed to ensure smooth and efficient operation of WTs and better serve society. This study uses heuristic optimization and FGA to optimize the layout of fans, and achieves cable layout optimization through PSO algorithm based on penalty function constraints. This study used a certain WF as an example for testing the effectiveness of the optimization algorithm. The data showed that the WT position based on FGA calculation was more optimal under different iteration times. After optimization, FGA can obtain the WT position with lower wake loss, which can further reduce the wake loss of the entire WF. The cable optimization results show that 4 out of 12 circuit cables have a lower load than before optimization, while 10 cables have a higher load than before optimization. There are 12 and 4 cables with optimized load greater than and less than before optimization for the 14 loop cables, and 10 cables with optimized load greater than before optimization for the 16 loop cables. Compared to the cable trench with 16 circuits, the optimized 14 circuit cable has less load reduction. After optimization, the total load of the 12 circuit cable is 5529.3A, which is 36.29A (0.65%) higher than before the optimization of the 16 circuit cable. This indicates that the proposed optimization algorithm has a certain effect on the layout of fans and cables. However, this study focuses on the analysis of environmental factors such as wind speed, wake, and terrain for the optimization algorithm of WT layout. In future research directions, further in-depth research is needed to improve the performance of optimization algorithms.

This study introduces an innovative method for optimizing the layout of wind turbines and wind farm cables, combining fuzzy genetic algorithm and particle swarm optimization with penalty function constraints. The results indicate that the layout design efficiency is improved, and the power generation and cable load distribution are enhanced. However, a key consideration for future applications is the scalability of algorithms for large wind farms. As the scale of wind farms expands, the complexity of optimization problems significantly increases, leading to longer computation times. The current method proposed in this article has been validated on medium-sized wind farms, but future work will focus on adjusting algorithms to handle larger datasets and wind farm layouts. Both FGA and PSO algorithms exhibit relatively high computational costs, especially with increasing population size and iteration times. To address this issue, parallel computing techniques or more effective heuristic methods can be explored to reduce runtime while maintaining optimization accuracy. However, simplifications in modeling environmental factors like terrain and wind speed pose a validity threat, and the study's focus on a

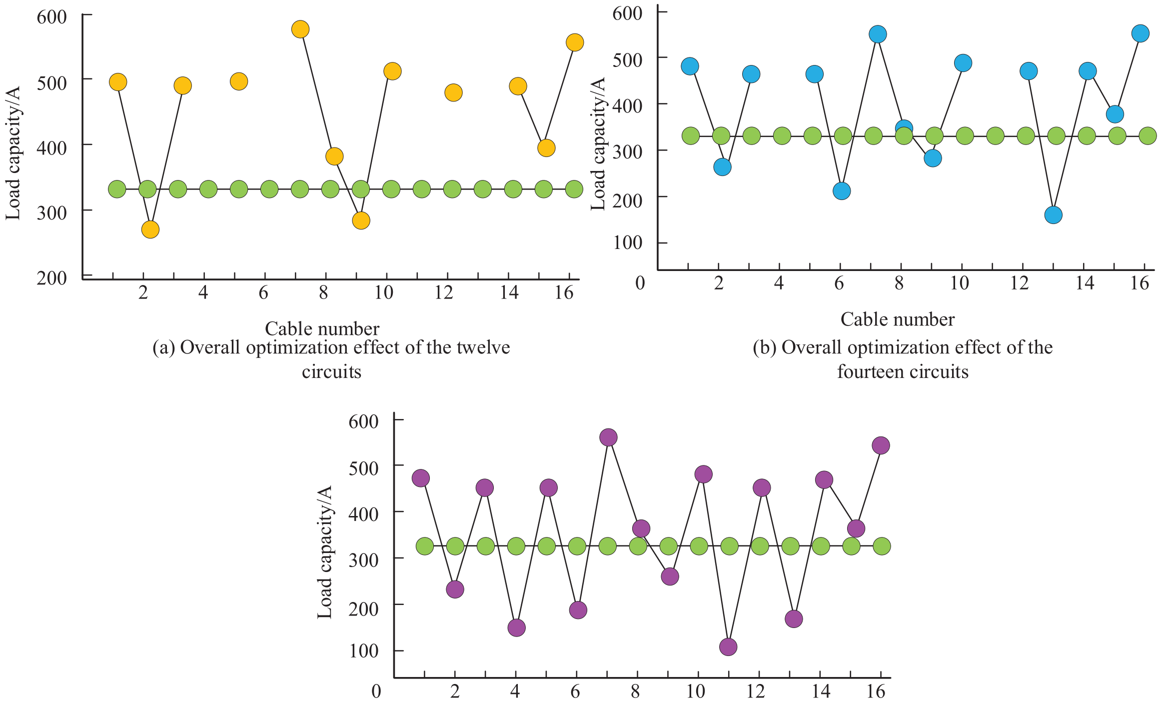

(a) Overall optimization effect of the twelve circuits

(b) Overall optimization effect of the fourteen circuits

(c) Overall optimization effect of the sixteen circuits

Fig. 8. The overall charge effect before and after optimizing different circuits.

specific wind farm in northeast China may limit generalizability. Future work should explore dynamic environmental conditions, renewable energy forecasting integration, and the scalability of these algorithms for large-scale projects, while addressing real-time operational constraints.

Funding

The authors did not receive any funding.

Conflicts of interest

There is no conflict of interest among the authors.

Data availability statement

Data will be available by corresponding author on reasonable request.

Author contribution statement

All authors have contributed equally in research work and the assessment of the outcomes and the writing of the manuscript.

Ethical approval

Not applicable.

Informed consent

Informed consent was obtained from all individual participants included in the study.
The participant has consented to the submission in this Journal.

References

1. P. Ziyaei, M. Khorasanchi, H. Sayyaadi, A. Sadollah, Minimizing the levelized cost of energy in an offshore wind farm with non-homogeneous turbines through layout optimization, Ocean Eng. **249**, 110859.1–110859.14 (2022)
2. C. Croonenbroeck, D. Hennecke, A comparison of optimizers in a unified standard for optimization on wind farm layout optimization, Energy **216**, 119244.1–119244.15 (2021)
3. S.R. Reddy, Wind Farm Layout Optimization (WindFLO): An advanced framework for fast wind farm analysis and optimization, Appl. Energy **269**, 115090.1–115090.13 (2020)
4. B. Kaya, E. Oguz, Investigation of layout optimization for offshore wind farms and a case study for a region in Turkey, Ocean Eng. **266**, 112807.1–112807.18 (2022)
5. F. Song, W. Guo, Global sensitivity and uncertainty evaluation of parameters for hybrid pumped storage-wind power generation system under wind speed disturbance, J. Energy Storage **132**, 117674 (2025)
6. S. Obara, R. Murofushi, Planning for local production and consumption of energy and electricity storage systems in regional cities, focusing on offshore wind power generation, Appl. Energy **395**, 126230 (2025)

7. I. Ulku, C. Alabas-Uslu, Optimization of cable layout designs for large offshore wind farms, Int. J. Energy Res. **44**, 6297–6312 (2020)
8. S.M. Masoudi, M. Baneshi, Layout optimization of a wind farm considering grids of various resolutions, wake effect, and realistic wind speed and wind direction data: a techno-economic assessment, Energy **244**, 123188.1–123188.16 (2022)
9. A.M. Ragab, A.S. Shehata, A.H. Elbatran, M.A. Kotb, Numerical optimization of hybrid wind-wave farm layout located on Egyptian North Coasts, Ocean Eng. **234**, 109260.1–109260.21 (2021)
10. Y. Wang, Z. Liu, H. Wang, Proposal and layout optimization of a wind-wave hybrid energy system using GPU-accelerated differential evolution algorithm, Energy **239**, 121850.1–121850.16 (2022)
11. S. Tao, Q. Xu, A. Feijóo et al., Nonuniform wind farm layout optimization: a state-of-the-art review, Energy **209**, 118339.1–118339.18 (2020)
12. S.R. Reddy, A machine learning approach for modeling irregular regions with multiple owners in wind farm layout design, Energy **220**, 119691.1–119691.12 (2020)
13. P. Petsagkourakis, F. Galvanin, Safe model-based design of experiments using Gaussian processes, Comput. Chem. Eng. **151**, 107339.1–107339.20 (2021)
14. K. Yetilmezsoy, P. Sihag, E. Kyan, B. Doran, A benchmark comparison and optimization of Gaussian process regression, support vector machines, and M5P tree model in approximation of the lateral confinement coefficient for CFRP-wrapped rectangular/square RC columns, Eng. Struct. **216**, 113106.1–113106.15 (2021)
15. H. Deng, A.C. To, Topology optimization based on deep representation learning (DRL) for compliance and stress-constrained design, Comput. Mech. **66**, 449–469 (2020)
16. J. Kim, J. Song, Reliability-based design optimization using quantile surrogates by adaptive gaussian process, J. Eng. Mech. **147**, 4021020.1–4021020.16 (2021)
17. T. AS, X. AQ, E. Andrés, B. Feijóo-Lorenzo, G. Zheng, J. Zhou, Optimal layout of a co-located wind/tidal current farm considering forbidden zones, Energy **228**, 120570.1–120570.16 (2021)
18. Z. Zhang, H. Dai, Y. Wang, Long-medium-short term nested operation model of hydro-wind-solar hybrid power system considering flood control, power generation, ecology and navigation, Energy **334**, 137705 (2025)
19. D. Pelosi, D.-A. Ciupageanu, A. Vaccaro, L. Barelli, Impact analysis of wind power generation on steady-state and transient stability of a national power system—The Romanian case study, Wind Energy Eng. Res. **3**, 100010 (2025)

Cite this article as: Xiaofeng Chen, Fei Rao, Yan Zhao, Adam Aakil, Optimization strategies for wind turbine and cable layout in wind farms, Int. J. Simul. Multidisci. Des. Optim. **16**, 19 (2025), https://doi.org/10.1051/smdo/2025024